applied sciences

IMPACT FACTOR 2.838

CITESCORE 3.7

Article

Microbiological Follow-Up of Bioreactor-Assisted Must Alcoholic Fermentation by Flow Cytometry

Federico Sizzano, Marie Blackford and Gilles Bourdin

Special Issue
Fermentation Technology in Food Production

Edited by
Dr. Ewa Jabłońska-Ryś and Dr. Aneta Sławińska

MDPI

https://doi.org/10.3390/app12189178

applied sciences

MDPI

Article

Microbiological Follow-Up of Bioreactor-Assisted Must Alcoholic Fermentation by Flow Cytometry

Federico Sizzano [1,*], Marie Blackford [1,2] and Gilles Bourdin [1]

[1] Oenology Research Group, Agroscope Research Center, Route de Duillier 50, 1260 Nyon, Switzerland
[2] Changins, Viticulture and Enology, HES-SO University of Applied Sciences and Arts of Western Switzerland, Route de Duillier 50, 1260 Nyon, Switzerland
* Correspondence: federico.sizzano@agroscope.admin.ch

Abstract: The monitoring of must fermentation in a bioreactor, in which the main physico-chemical parameters are tightly controlled, can provide useful analytical information transferable to winemaking on a larger scale. In this experiment, we followed the growth of *Saccharomyces cerevisiae* during the bioreactor-assisted alcoholic fermentation of a *Chasselas* must by means of flow cytometry. We used fluorescent dyes and volumetric counting to monitor cell viability and concentration for two weeks. Our study suggests that the use of flow cytometry during bioreactor-assisted alcoholic fermentation provides various types of information—viz., cell viability, number and function—in a timely manner, and that the process can therefore be used effectively to inform experimentation at this scale.

Keywords: yeast; alcoholic fermentation; bioreactor; flow cytometry

Citation: Sizzano, F.; Blackford, M.; Bourdin, G. Microbiological Follow-Up of Bioreactor-Assisted Must Alcoholic Fermentation by Flow Cytometry. *Appl. Sci.* **2022**, *12*, 9178. https://doi.org/10.3390/app12189178

Academic Editors: Ewa Jabłońska-Ryś and Aneta Sławińska

Received: 9 August 2022
Accepted: 9 September 2022
Published: 13 September 2022

1. Introduction

Bioreactors, which allow for the continuous control of the main alcoholic fermentation (AF) parameters, represent a useful tool in experimental winemaking to guide in-cellar experimentation at a higher scale. The main parameters monitored by bioreactors include temperature, pH, oxygen concentration and pressure in the fermentation chamber. Variations in these parameters have important effects on the fermentation process, as shown by several researchers. For example, Liu et al. [1], studied the pH variation in an artificial must and observed that low initial pH impacted the outcome of fermentation in terms of sugar consumption, biomass production and final alcohol content. Similarly, Beltran et al. [2] showed that high temperatures boosted the fermentation rate but could have profound effects on yeast metabolism and final aroma profile. Finally, Guerrini et al. [3] observed that increased pressure during fermentation led to a higher concentration of esters, usually associated with the fruity attribute in wine. Changes in these parameters primarily affect the metabolism and biology of the yeast responsible of fermentation, including both *Saccharomyces cerevisiae* (SC) and *non-Saccharomyces* species. Thus, it is of utmost importance to have a method in place that allows the dynamics of yeast growth to be tracked during bioreactor-assisted fermentation. Such a method should not only give information about the viability of the yeast but also provide functional details that, in turn, could be correlated to the physico/chemical parameter(s) under investigation (e.g., pH, temperature or pressure). Moreover, this method should provide results in a timely manner, to allow for consistent follow-up after experimentation. One of the best candidates to fill this role is flow cytometry (FCM), a single-cell, fluorescence-based technique, widely used in biomedicine [4]. FCM has been used to evaluate the growth of a microorganism of interest in bioreactor-assisted fermentation in various fields including antibody [5], bioethanol [6], and amino-acid production [7].

In winemaking, FCM has been applied to follow AF at the bench scale [8–12]; however, to the best of our knowledge, there is a limited amount of data on FCM as a method to follow the yeast growth in bioreactor-assisted fermentation [13]. Thus, we aimed to perform a 20 L-vinification trial by means of an automated bioreactor and to evaluate the yeast

growth dynamics using FCM. We applied and compared two different staining protocols to measure the yeast's physiological state. Moreover, we performed FCM data analysis in a classical operator-dependent manner, as well as using an unsupervised software algorithm, to capture all the complexity within the sample in a single two-dimensional (2D) map.

2. Materials and Methods

2.1. Must

Twenty litres of frozen *Chasselas* must (from a 2021 vintage) were used. Upon arrival in the cellar, grapes were crushed, pressed and treated with sulphur dioxide (SO_2; 50 mg/L), and the enzyme LittoZym Kler P (1 g/hL) was added prior to a 36-h settling process. Clear white juice was frozen at −20 °C in sterilised jerrycans. Two days before experimentation, the must was brought to a temperature of 4 °C and then to room temperature, allowing for progressive and gentle thawing.

2.2. Bioreactor-Assisted Fermentation

The experiment was carried out in a Bionet F2-30 bioreactor (Bionet, Fuente Alamo, Spain) equipped with a double-wall tank, allowing the control of the inner chamber temperature, and with an airflow rate/pressure control. The yeast (*Saccharomyces cerevisiae*, Lallemand Lalvin CY 3079, Blagnac Cedex, France) was rehydrated following the manufacturer's protocol and added to the must at a final concentration of 20 g/hL. Then, the inoculated must was poured into the reaction chamber, which had been sterilised following the manufacturer specifications. The temperature was set at 20 °C for the entire fermentation process without adding further pressure in the reaction chamber (the maximum set pressure allowed was 0.1 barg). The precise temperature control was subject to the continuous agitation of the must by means of a rotor in the internal chamber (speed: 50 rpm, 2 × 6 blade Rushton impellers). A closed circuit and a heat exchanger enabled automatic heating and cooling through the circulation of hot water (if resistance was active) or cold water from a cryostat to the jacket. Sampling for densitometry and FCM analysis was carried out using a dedicated sampling port, coupled with an external steam-producing unit for sterilisation. Once per day, the sampling port was sterilised, and 5 to 10 mL of must in the process of fermentation was collected in a 15 mL Falcon polypropylene sterile tube. After sample collection, the port was closed, and it was then purged and sterilised.

2.3. Densitometry

Densitometry was carried out using an Anton Paar DMA 35 handheld density meter (Anton Paar AG, Buchs, Switzerland). Density values expressed in Oechsle degrees were recorded daily. Fermentation was considered finished when consistent negative density values, indicating sugar consumption and the presence of alcohol, were recorded for at least two consecutive days.

2.4. Sample Staining and FCM

FCM analysis was carried out once per day until the end of fermentation. For this purpose, 50 µL of must was diluted in 950 µL of phosphate buffer saline (PBS). Three samples were prepared for analysis: one unstained sample and two samples stained with two different protocols to assess yeast viability. In the first protocol SYBR Green (Fisher Scientific, Waltham, MA, USA) was diluted 10,000 times, whereas in the second protocol 5-Carboxyfluorescein-diacetate, acetoxymethyl-ester (CFDA-AM; Fisher Scientific) was added to a final concentration of 2 µM. To visualize the dead cells, defined as those with a compromised cell membrane, the impermeant dye propidium iodide (PI, Fisher Scientific) was added to a final concentration of 0.05 µg/mL in the first protocol and 0.5 µg/mL in the second protocol. Stained samples were incubated for 15 min at room temperature and acquired by means of a MACSQuant Cell Analyzer (Miltenyi Biotech, Solothurn, Switzerland) equipped with 405 nm, 488 nm and 640 nm laser lines and capable of volumetric cell counting. Instrument performance was checked daily by means of the

MACS Quant Calibration Beads (Miltenyi Biotech) and the dedicated software option of the MACSQuant acquisition programme. In total, 25 µL of diluted samples were acquired, and fluorescence emissions were collected by means of specific band-pass filters. SYBR Green + PI- and CFDA + PI- cells were defined as live cells, whereas all PI+ cells were defined as dead cells. CFDA + PI+ cells (usually a small percentage of the total) were considered damaged. Results were expressed as number of live/dead cells/mL (for each protocol), as percentage of live/dead cell in the parental gate (i.e., scatter gate) and as median fluorescence intensity (MFI) for CFDA. Classical dot plot-based analysis [4] was carried out using FlowLogic (Flow Logic Software, Victoria, Australia), whereas unsupervised analysis using t-distributed Stochastic Neighbor Embedding (t-SNE)—the dimensionality reduction algorithm—was performed using the FCS Express software package (DeNovo Software, Pasadena, CA, USA). Statistical analysis was performed using the Prism (Graphpad, San Diego, CA, USA) and MedCalc (MedCalc Software, Ostend, Belgium) software packages.

3. Results

3.1. Background Evaluation and Cell Population Visualisation

Grape must is a complex chemical matrix containing different molecular species as well as lipid particles and indigenous microorganisms. Such complexity can interfere with the FCM analysis, sometimes leading to a misinterpretation of results. Thus, we analysed the must before and after yeast inoculation, to define the correct cell population and differentiate it from the background. Figures 1 and 2 show the FCM analysis of the samples before and after yeast inoculation for both protocols, along with the gating strategy.

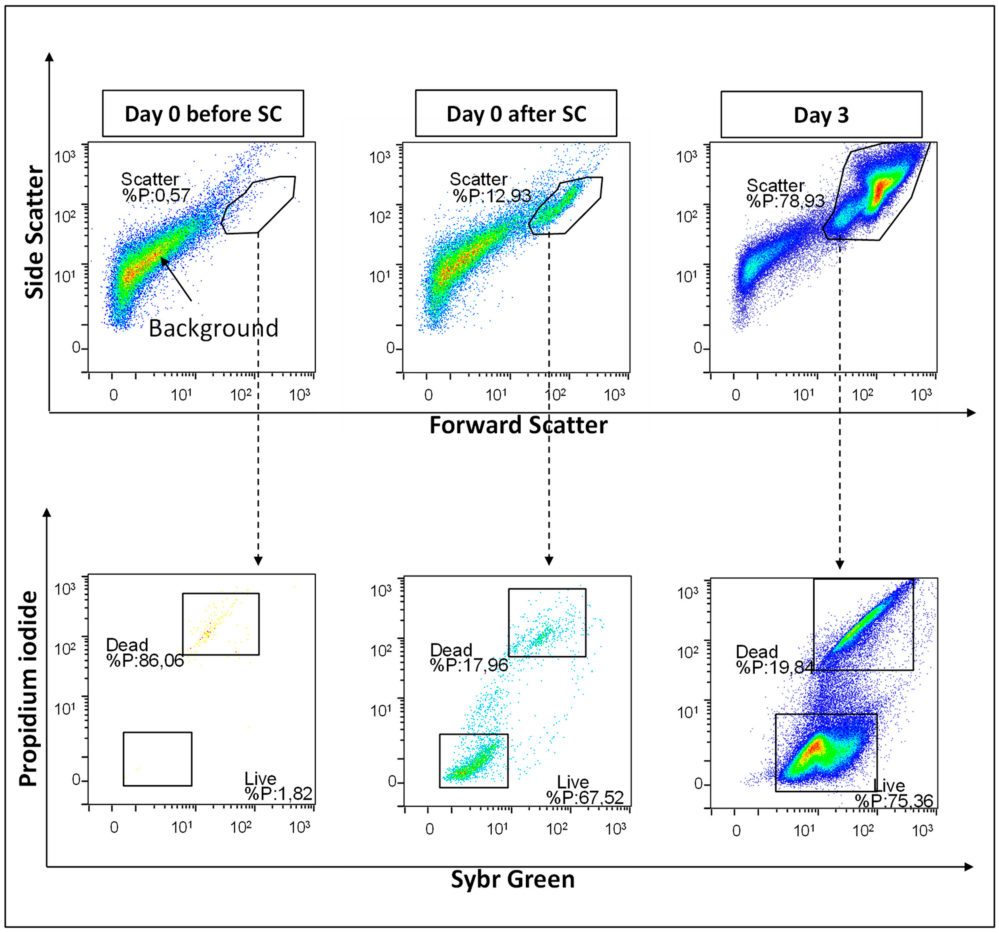

Figure 1. FCM analysis and gating strategy for the SYBR-PI protocol. The different colours indicate the cell density (blue/green = low cell density; yellow/red = high cell density). Before SC: must before SC inoculation; after SC: must after SC inoculation.

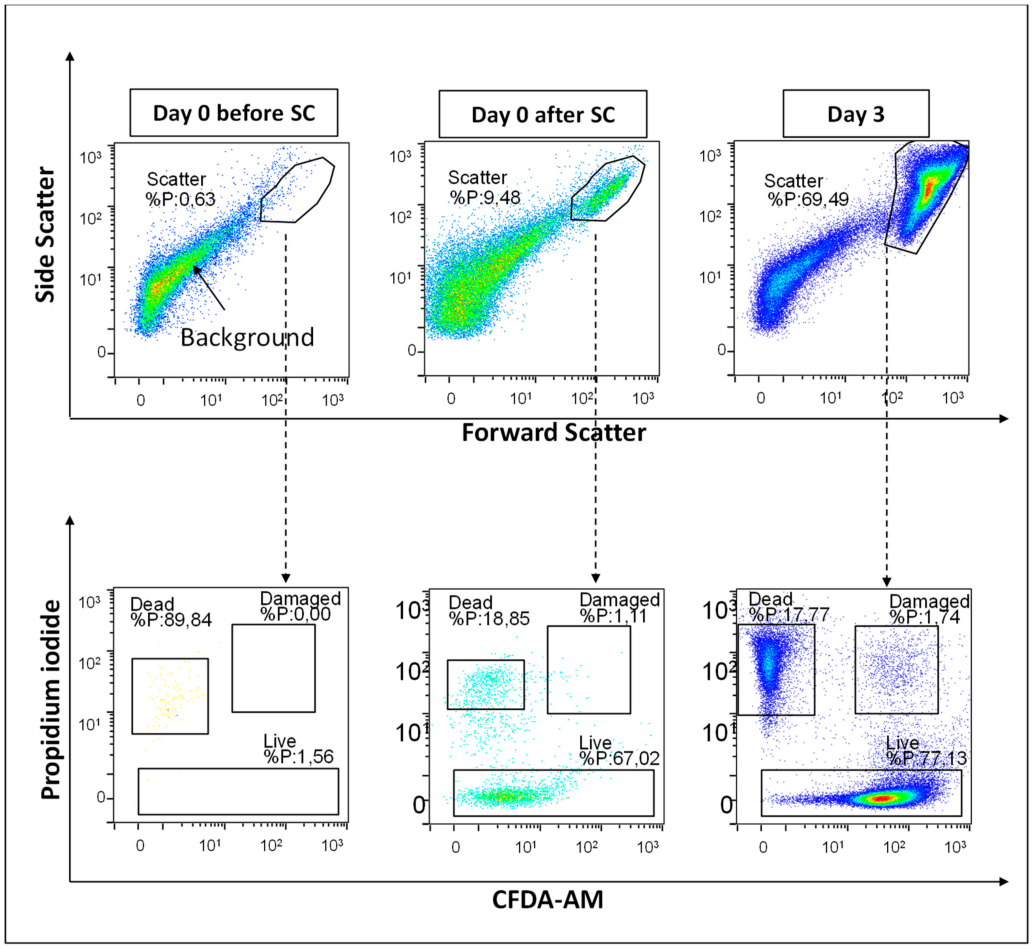

Figure 2. FCM analysis and gating strategy for the CFDA-PI protocol. The different colours indicate the cell density (blue/green = low cell density; yellow/red: high cell density). Before SC: must before SC inoculation; after SC: must after SC inoculation.

The must samples contained a high number of unknown events visualised as a smear of dots encompassing different Forward (FSC) and Side Scatter (SSC) values (identified as "Background" in Figures 1 and 2). However, such events did not appear to be stained specifically by any of the dye used (data not shown). After yeast inoculation, we clearly observed a cluster of events with high FSC/SSC values, which was consistent with the yeast population, and was either not present in the must that had been not inoculated, or at a very low level (see upper plots in Figures 1 and 2). Thus, we proceeded to the gating strategy to visualise the different fluorescence parameters only in the scatter gate (see lower plot in Figures 1 and 2). Cell concentration increased, as expected, on day 3 (Figures 1 and 2) and the scatter and fluorescence parameters (especially CFDA) also changed, as a consequence of the increased fermentative metabolism.

3.2. Yeast Growth Dynamics Follow up with the SYBR-PI and CFDA-PI Protocols

The FCM results showed a pattern of progressive decrease in the cell number of live cells starting from the days 3–5 until the end of the follow-up on day 14, consistent with the sugar consumption as measured by densitometry. Conversely, the number of dead cells increased progressively from days 3–5 to the end of day 14. These trends were consistent between the two protocols (Figure 3A,C). The analysis of the percentage of live and dead cells provided similar results for both protocols. However, the results of this analysis showed a smoother profile of both live and dead cells throughout the fermentation process, as compared to that found when analysing absolute numbers (Figure 3B,D).

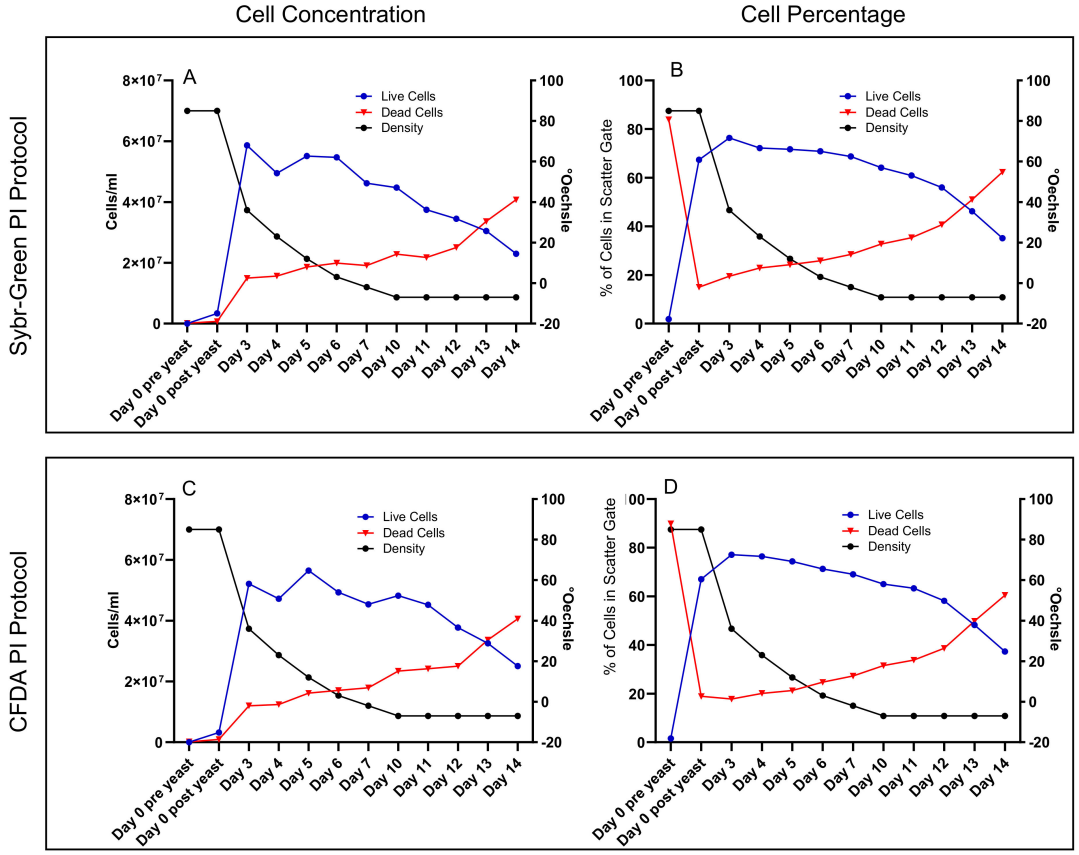

Figure 3. Yeast growth dynamics by FCM as defined by the two staining protocols, SYBR-PI and CFDA-PI. (**A**,**C**) show the concentration of live and dead cells, whereas (**B**,**D**) show the percentage of cells in the scatter gate (i.e., parent gate).

3.3. Protocol Comparison

Next, we compared the two protocols for all the parameters evaluated (i.e., live and dead cells concentration, and live and dead cell percentage). The results of a Passing Bablok regression analysis showed good regression values for the two methods for all the conditions. Table 1 shows the slope and intercept values with the respective 95% confidence interval (CIs). Moreover, we used the graphical Bland–Altman plot method, identifying SYBR-PI as method 1 and CFDA-PI as method 2. The results showed that for live cell concentrations, the two methods showed greater differences with increasing cell concentration; however, for dead cell concentrations, the major differences were found only at low cell numbers (Figure 4A,B).The live cell percentage results showed a narrow interval of agreement and a low bias, despite the presence of an outlier at the limits of the 95% CI. In general, the CFDA-PI protocol gave higher values of live cells than did SYBR-PI protocol. For dead cell percentages, the results showed the opposite situation (Figure 4C,D).

Table 1. Results from Passing Bablok regression.

Parameter	Intercept	Slope	CI Intercept	CI Slope
live cells/mL	3,064,803	0.9299	−447,412.2 to 12,309,498.2	0.6911 to 1.0830
dead cells/mL	−2,877,204.1	1.0864	−6,912,695.8 to 98,702.5	0.9603 to 1.2708
live cell%	0.6956	1.0139	−1.4830 to 4.9771	0.9363 to 1.0603
dead cell%	−1.5243	1.0037	−4.6551 to 0.6088	0.9383 to 1.0968

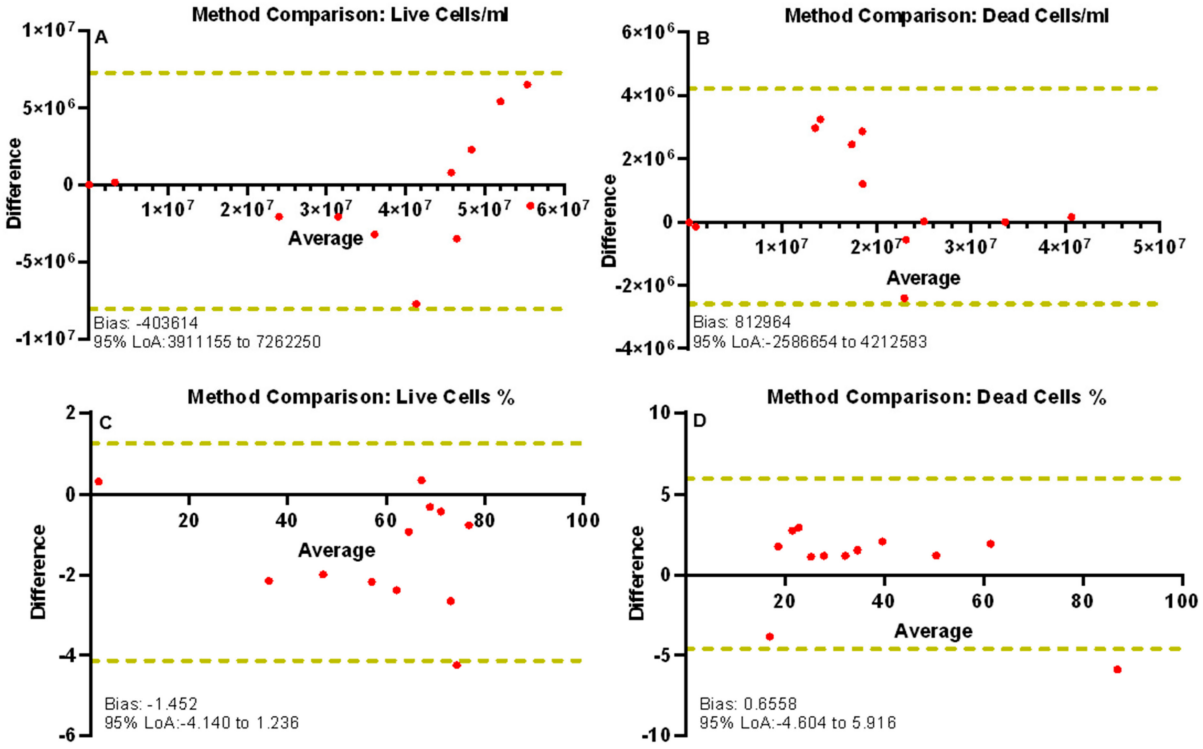

Figure 4. Bland Altman plots for method comparison. In this figure, x values represent the average of the two measures (i.e., [SYBR-PI value + CFDA-PI value]/2), whereas y values represent the difference between the two (i.e., SYBR-PI value − CFDA-PI value); bias indicates the average of the differences between the two methods. LoA: limit of acceptance. (**A**–**D**) method comparison for each parameter under investigation. (**A**) live cells/mL; (**B**) dead cells/mL; (**C**) % of live cells; (**D**) % of dead cells.

3.4. CFDA Fluorescence Changes during Fermentation

During fermentation, we observed a progressive decrease of CFDA MFI in the live population. This change was consistent throughout the follow-up period and correlated with sugar consumption as measured by densitometry. We quantified such correlation from day 3, and our results showed a high Spearman coefficient (r = 0.92, $p < 0.001$; Figure 5).

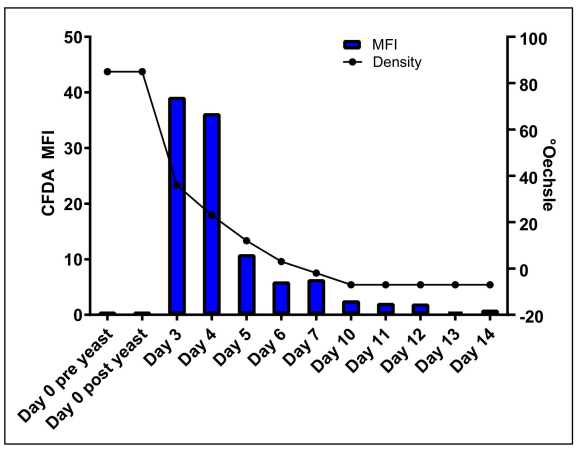

Figure 5. CFDA MFI and density decrease during fermentation.

3.5. Unsupervised FCM Analysis of Fermentation: Example Using CFDA Protocol

Finally, we ran the t-SNE algorithm including four parameters: FSC, SSC, CFDA and PI to visualise in one plot the complexity of the sample. As an example, we selected the

t-SNE analysis plots from day 7, which show the appearance of at least two big cell clusters (Figure 6D) that were identified, by means of a classical 2D analysis (Figure 6C), as live cells (blue cluster) or dead cells (red cluster). The damaged cells were also clearly defined, shown in the green cluster (Figure 6D). However, we observed that the cluster containing the live cells could have been divided into at least two sub-clusters (see the arrow in Figure 6D). Therefore, we drew two additional gates in the t-SNE plot (Figure 6E, gates 1–2) and observed their cell content in two more CFDA-PI plots. Our results revealed two partially overlapping populations displaying different CFDA levels, not directly recognisable in the original 2D CFDA-PI dot plot (Figure 6E–I).

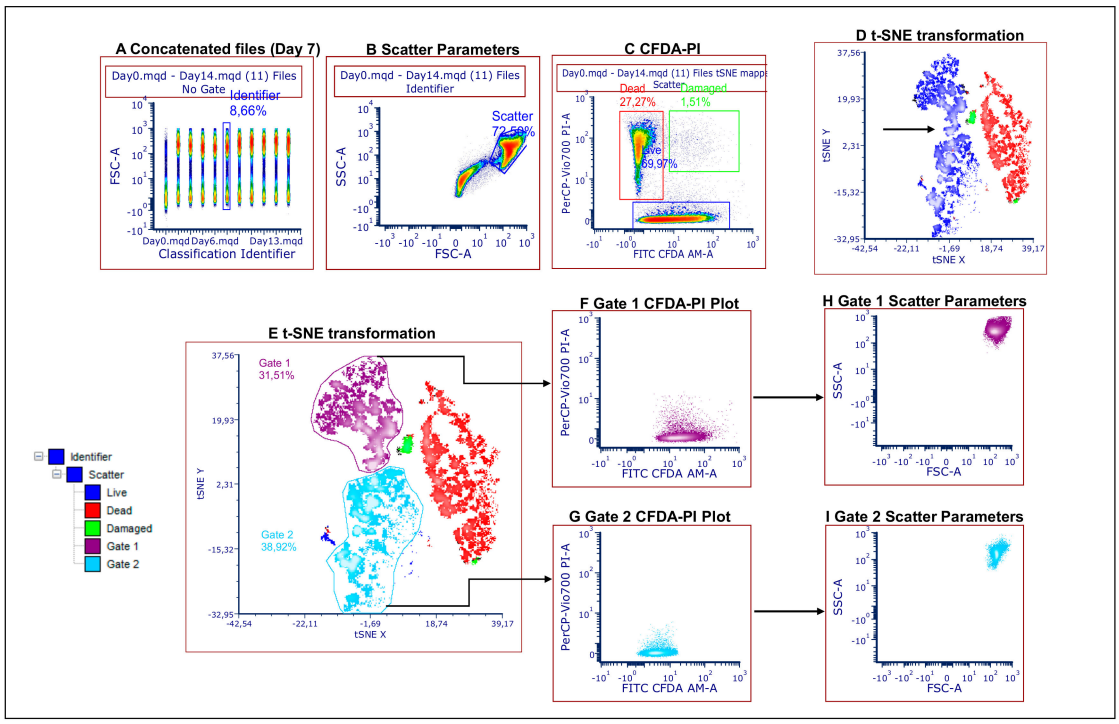

Figure 6. Unsupervised analysis and exemplative t-SNE and 2D plots from day 7. (**A**) All FCS files are concatenated in a single file for t-SNE analysis. The results from day 7 are further displayed (see events in the "Identifier" gate). (**B**) Scatter dot plot. (**C**) Dot plot identifying live, dead and damaged cells by CFDA-PI staining. (**D**) The t-SNE transformation plot. Note that the main populations from (**C**) are easily identifiable in the t-SNE plot: blue cluster = live cells, red cluster = dead cells and green cluster = damaged cells. (**E**) The t-SNE plot and gating of two subclusters. (**F**–**I**) The CFDA-PI and scatter profiles of cells within gates 1 and 2.

4. Discussion

In the present work we used FCM to examine the growth dynamics of SC in the bioreactor-assisted fermentation of a *Chasselas* must. The temperature and pressure were kept constant for the duration of the experiment, trying to mimic the conditions typically used in the cellar. The FCM data precisely illustrated the classical kinetics of must fermentation, and this was observed in terms of both the percentages and the absolute counts. The agitation in the bioreactor maintained a homogeneous yeast suspension, and this represents ideal conditions for a consistent sampling and downstream FCM analysis. However, the fermenting must is not usually subject to continuous stirring and future experimentation should take this aspect under consideration—for example by stirring only a few minutes before sampling—to avoid any unwanted effects of long-term agitation.

It is important to underline that in this study, the FCM results—both counts and percentages—were obtained in a very short time. In fact, it took only half an hour from must sampling to the final acquisition at the analyser, including the transportation of the sample to the laboratory. Indeed, FCM can represent a quasi-online analytical tool. As such,

we also applied a method that did not include centrifugation or filtration steps, to keep the sample as pristine as possible and to save time. The choice of a 1:20 dilution was made in the first staining trials at the beginning of fermentation and proved to be effective for FCM acquisition, in order to avoid doublet formation or clumping, as revealed by the SSC-Area (SSC-A) versus SSC-Height (SSC-H) dot plot for doublet discrimination (data not shown).

We also applied two protocols that have been widely used in microbiology as well as in oenology. The first protocol contained SYBR Green, a stoichiometric DNA-specific dye applied in oenology to study yeast cell cycle [14]. The second protocol contained a fluorescein derivative, CFDA-AM. Such derivatives have been widely used in FCM to follow both alcoholic and malolactic fermentation [8,10,13,15]. We chose to use CFDA-AM because it can be loaded in the cell at lower concentrations compared to those used with the other derivatives, as the AM group makes the dye more cell permeable. Overlapping yeast growth kinetics in the bioreactor were appreciated in both the SYBR-PI and the CFDA-PI protocols, and this was true for both cell counts and percentages. The results from the method comparison suggested that the two methods are generally in agreement, as almost all the measurements were within the LoA with acceptable bias values. The biggest differences were found when analysing the cell concentrations. However, they did not affect the overall kinetics.

Thus, the two methods can be used interchangeably with respect to the experimental design. For future analyses, one possibility could be merging the two methods, changing the type of DNA dye regarding the fluorescence excitation/emission profile. Such configuration would provide a particular benefit in high-background samples, in which DNA dye could help in extracting the specific signal from the background for proper CFDA analysis.

CFDA-based protocols offer more functional information compared to protocols using DNA-dyes, because CFDA MFI has been related to the esterase activity and, thus, to the general metabolic activity of the cell [16]. We observed that the CFDA MFI of the live population (defined as CFDA + PI-) decreased throughout the fermentation process. It is known that fluorescein derivatives such as CFDA are pH sensitive, and the amount of fluorescence emitted is directly proportional to the pH value. Interestingly, Viana et al. [17] observed that a decrease in yeast intracellular pH (ipH) occurred in the late stationary phase of fermentation. In our case, this phase should correspond to day 5, in which we started to observe decreasing viability. It is noteworthy that day 5 was also the day on which we observed the most dramatic decrease in CFDA MFI. Therefore, we could hypothesise that the observed decrease of CFDA fluorescence was driven by ipH changes. However, because we did not directly measure the enzymatic activity, we could not rule out a direct effect of ipH on esterase activity, the reduction of which could also have led to an overall decrease of CFDA fluorescence [18]. Moreover, it is interesting to note that even after inoculation, the yeast cells displayed low CFDA MFI, although the majority of the cells were PI-, indicating that the cells did not have their membranes compromised (see "day 0" in Figure 2). This observation could be explained by the fact that the yeasts were just rehydrated and needed to rewire their metabolism in the new medium. More likely, the yeast cells were not yet capable of bringing the ipH close to neutrality and this possibly affected the CFDA fluorescence emission.

From the classical operator-dependent analysis, the population of live cells appeared to be affected by the loss of CFDA fluorescence as a whole, and the distribution of fluorescence values followed a Gaussian distribution (data not shown). However, we could not rule out the presence of functional, discrete clusters possessing different activities during the fermentation process. Thus, to investigate possible "hidden clusters", at least from an FCM perspective, we applied unsupervised analysis using the t-SNE algorithm to capture the sample complexity, and to observe the structure of (putative) sub-populations. Our results showed three clusters: two big clusters and one small cloud in the centre. Gating the CFDA-PI plots made recognisable the live cells, the dead cells and the small cluster of damaged cells. We observed, however, that in the t-SNE transformation plot the live cell cluster could be furtherly divided into two sub-clusters separated by a bottleneck end. Thus,

we gated these clusters on the CFDA-PI plot and recognised two partially overlapping cell populations also displaying different scatter profiles. It is tempting to speculate that these populations could have different metabolic activity levels and, thus, contribute to fermenting the remaining sugars at different rates. However, it must be emphasised that this was a purely post-analytical attempt to further understand the variability of the yeast population in fermentation and that the results of the t-SNE analysis in terms of new and interesting clusters should be validated with other methods, including cell sorting and functional assays.

Although in this paper we mainly present results from an observational study, we also suggest that FCM can be used as a quick and robust tool to follow up the experiments at the bioreactor scale. The staining protocols used are easy to apply, and the sample preparation has been kept as simple as possible. Results can already be seen after 15–30 min, and, thus, the operator can follow-up on the experiments in a timely manner. In the future, FCM can be used to follow yeast (or bacteria) growth in dedicated assays, for example focusing on pH (i.e., for acidifier yeasts) or pressure changes (e.g., their effect on indigenous yeast). It is hoped that new fluorescent reagents specifically designed to follow metabolic pathways of interest will be developed. Lastly, the application of unsupervised algorithms will be of the utmost importance when digging deeper into the functional complexity of the fermentation.

Author Contributions: Conceptualization, F.S., M.B. and G.B.; methodology, F.S., M.B. and G.B.; validation, F.S.; formal analysis, F.S.; investigation, F.S. and M.B; resources, F.S., M.B. and G.B.; writing—original draft preparation, F.S.; writing—review & editing, F.S., M.B. and G.B.; visualization, F.S.; supervision, G.B. All authors have read and agreed to the published version of the manuscript.

Funding: This research received no external funding.

Institutional Review Board Statement: Not applicable.

Informed Consent Statement: Not applicable.

Data Availability Statement: The data presented in this study are available on reasonable request from the corresponding author.

Acknowledgments: The Authors would like to thank Regula Wolz Gysi, Head of the Language Service, Agroscope, for her help in editing the language of this manuscript.

Conflicts of Interest: The authors declare no conflict of interest.

References

1. Liu, X.; Jia, B.; Sun, X.; Ai, J.; Wang, L.; Wang, C.; Zhao, F.; Zhan, J.; Huang, W. Effect of Initial pH on Growth Characteristics and Fermentation Properties of *Saccharomyces cerevisiae*. *J. Food Sci.* **2015**, *80*, M800–M808. [CrossRef] [PubMed]
2. Beltran, G.; Novo, M.; Guillamón, J.M.; Mas, A.; Rozès, N. Effect of Fermentation Temperature and Culture Media on the Yeast Lipid Composition and Wine Volatile Compounds. *Int. J. Food Microbiol.* **2008**, *121*, 169–177. [CrossRef] [PubMed]
3. Guerrini, L.; Masella, P.; Angeloni, G.; Sacconi, A.; Calamai, L.; Parenti, A. Effects of a Small Increase in Carbon Dioxide Pressure during Fermentation on Wine Aroma. *Foods* **2020**, *9*, 1496. [CrossRef] [PubMed]
4. Robinson, J.P. Flow Cytometry: Past and Future. *Biotechniques* **2022**, *72*, 159–169. [CrossRef] [PubMed]
5. Lin, S.; Shen, Z.; Zha, D.; Sharkey, N.; Prinz, B.; Hamilton, S.; Pavoor, T.V.; Bobrowicz, B.; Shaikh, S.S.; Rittenhour, A.M.; et al. Selection of *Pichia pastoris* Strains Expressing Recombinant Immunoglobulin G by Cell Surface Labeling. *J. Immunol. Method.* **2010**, *358*, 66–74. [CrossRef] [PubMed]
6. Vees, C.A.; Veiter, L.; Sax, F.; Herwig, C.; Pfugl, S. A Robust Flow Cytometry-Based Biomass Monitoring Tool Enables Rapid At-Line Characterization of *S. cerevisiae* Physiology During Continuous Bioprocessing of Spent Sulfite Liquor. *Anal. Bioanal. Chem.* **2020**, *412*, 2137–2149. [CrossRef] [PubMed]
7. Liu, Y.; Li, Q.; Zheng, P.; Zhang, Z.; Liu, Y.; Sun, C.; Cao, G.; Zhou, W.; Wang, X.; Zhang, D.; et al. Developing a High-Throughput Screening Method for Threonine Overproduction Based on an Artificial Promoter. *Microb. Cell Fact.* **2015**, *14*, 121. [CrossRef] [PubMed]
8. Malacrinò, P.; Zapparoli, G.; Torriani, S.; Dellaglio, F. Rapid Detection of Viable Yeasts and Bacteria in Wine by Flow Cytometry. *J. Microbiol. Methods* **2001**, *45*, 127–134. [CrossRef]

9. Branco, P.; Monteiro, M.; Moura, P.; Albergaria, H. Survival Rate of Wine-Related Yeasts During Alcoholic Fermentation Assessed by Direct Live/Dead Staining Combined with Fluorescence in situ Hybridization. *Int. J. Food Microbiol.* **2012**, *158*, 49–57. [CrossRef] [PubMed]
10. Bouchez, J.C.; Cornu, M.; Danzart, M.; Leveau, J.Y.; Duchiron, F.; Bouix, M. Physiological significance of the cytometric distribution of fluorescent yeasts after viability staining. *Biotechnol. Bioeng.* **2004**, *86*, 520–530. [CrossRef] [PubMed]
11. Petitgonnet, C.; Klein, G.L.; Roullier-Gall, C.; Schmitt-Kopplin, P.; Quintanilla-Casas, B.; Vichi, S.; Julien-David, D.; Alexandre, H. Influence of Cell-Cell Contact Between *L. thermotolerans* and *S. cerevisiae* on Yeast Interactions and the Exo-Metabolome. *Food Microbiol.* **2019**, *83*, 122–133. [CrossRef] [PubMed]
12. Cisilotto, B.; Scariot, F.J.; Schwarz, L.V.; Kaue Mattos Rocha, R.; Longaray Delamare, A.P.; Echeverrigary, S. Yeast Stress and Death Caused by the Synergistic Effect of Ethanol and SO_2 During the Second Fermentation of Sparkling Wines. *OENO One* **2021**, *4*, 51–71. [CrossRef]
13. Bouix, M.; Leveau, J.Y. Rapid Assessment of Yeast Viability and Yeast Vitality During Alcoholic Fermentation. *J. Inst. Brew.* **2001**, *107*, 217–225. [CrossRef]
14. Palomba, E.; Tirelli, V.; de Alteriis, E.; Parascandola, P.; Landi, C.; Mazzoleni, S.; Sanchez, M. A Cytofluorimetric Analysis of a *Saccharomyces cerevisiae* Population Cultured in a Fed-Batch Bioreactor. *PLoS ONE* **2021**, *16*, e0248382. [CrossRef] [PubMed]
15. Guzzon, R.; Larcher, R. The Application of Flow Cytometry in Microbiological Monitoring during Winemaking: Two Case Studies. *Ann. Microbiol.* **2015**, *65*, 1865–1878. [CrossRef]
16. Longin, C.; Petitgonnet, C.; Guillox-Benatier, M.; Rousseaux, S.; Alexandre, H. Application of Flow Cytometry to Wine Microrganisms. *Food Microbiol.* **2017**, *62*, 221–231. [CrossRef] [PubMed]
17. Viana, T.; Loureiro-Dias, M.C.; Loureiro, V.; Prista, C. Peculiar H^+ Homeostasis of *Saccharomyces cerevisiae* During the Late Stages of Wine Fermentation. *Appl. Environ. Microbiol.* **2012**, *78*, 6302–6308. [CrossRef] [PubMed]
18. Bouix, M.; Ghorbal, S. Rapid Assessment of *Oenococcus oeni* Activity by Measuring Intracellular pH and Membrane Potential by Flow Cytometry, and its Application to the More Effective Control of Malolactic Fermentation. *Int. J. Food Microbiol.* **2015**, *193*, 139–146. [CrossRef] [PubMed]